

1           **Remarkable weakness against cleavage stress for YBCO-coated**  
2           **conductors and its effect on the YBCO coil performance**

3  
4  
5           Y. Yanagisawa<sup>1,2,3</sup>, H. Nakagome<sup>2</sup>, T. Takematsu<sup>1,4</sup>, T. Takao<sup>4</sup>,  
6           N. Sato<sup>5</sup>, M. Takahashi<sup>1,5</sup>, and H. Maeda<sup>1,5</sup>

7  
8       <sup>1</sup>Systems and Structural Biology Center, RIKEN, Yokohama, 230-0045, Japan

9       <sup>2</sup>Graduate School of Engineering, Chiba University, Chiba, 236-8522, Japan

10      <sup>3</sup>Reserch Fellow of the Japan Society for the Promotion of Science, Tokyo, 102-8472,

11      Japan

12      <sup>4</sup>Faculty of Science and Technology, Sophia University, Tokyo, 102-8554, Japan

13      <sup>5</sup>Graduate School of Yokohama City University, Yokohama, 230-0045, Japan

14  
15      Corresponding author:

16      Name: Hideaki Maeda

17      Phone: +81-045-508-7211

18      Fax: +81-045-508-7360

19      E-mail address: maeda@jota.gsc.riken.jp

20

1 **Abstract**

2 Cleavage strength for an YBCO-coated conductor at 77 K was  
3 investigated with a model experiment. The nominal cleavage strength for an  
4 YBCO-coated conductor is extremely low, typically 0.5 MPa. This low nominal  
5 cleavage strength is due to stress concentration on a small part of the YBCO-coated  
6 conductor in cleavage fracture. Debonding by the cleavage stress occurs at the interface  
7 between the buffer layer and the Hastelloy substrate. The nominal cleavage strength for  
8 a slit edge of the conductor is 2.5-times lower than that for the original edge of the  
9 conductor; cracks and micro-peel existing over the slit edge reduce the cleavage  
10 strength for the slit edge. Cleavage stress and peel stress should be avoided in coil  
11 winding, as they easily delaminate the YBCO-coated conductor, resulting in substantial  
12 degradation of coil performance. These problems are especially important for epoxy  
13 impregnated YBCO-coated conductor coils. It appears that effect of cleavage stress and  
14 peel stress are mostly negligible for paraffin impregnated YBCO-coated conductor coils  
15 or dry wound YBCO-coated conductor coils.

16

17

18

- 1 **Keywords:**
- 2 YBCO-coated conductor
- 3 YBCO coil
- 4 Stress concentration
- 5 Cleavage
- 6 Peel
- 7 Delamination
- 8 Degradation
- 9 Stress analysis
- 10 Critical current
- 11

## 1 **1. Introduction**

2           A YBCO-coated conductor tolerates axial tensile stress as high as, and possibly  
3 higher than 700 MPa [1-3]. This is much higher than comparable stress numbers for  
4 both 1G high temperature superconductors (HTS) [4] and low temperature  
5 superconductors (LTS) [5]. If we take advantage of YBCO-coated conductors, we can  
6 increase current density in the superconducting coils thus reducing their volumes.[6]  
7 However, an YBCO-coated conductor is delaminated and degraded by a transverse  
8 tensile stress of 10-20 MPa.[7] Such anisotropic stress tolerance of the YBCO-coated  
9 conductor affects the coil performance.

10           In a previous paper [8], we demonstrated that an epoxy impregnated  
11 YBCO-coated conductor double-pancake coil showed substantial degradation in coil  
12 performance. This was because part of the conductor was delaminated. This was  
13 interpreted as excessive transverse stress; i.e. the cumulative transverse (radial) stress,  
14 12 MPa, developed during epoxy cure [9] and cool down [8] degraded the conductor in  
15 the coil winding because it exceeded the tensile transverse strength, 10-20 MPa, of the  
16 YBCO-coated conductor [7]. Xie et al. [10] recently reported the transverse tensile  
17 strength for commercial YBCO-coated conductors as 40-100 MPa. Considering such  
18 higher transverse tensile strengths for recent conductors, it is necessary to examine

1 additional sources of stress in the coil winding.

2 YBCO-coated conductors used in the previous work [8] were made up of  
3 numbers of layers. [1] This can be modeled as an adhesive lap joint, where two  
4 adherends of a copper/Hastelloy layer and a silver/copper layer are bonded by the brittle  
5 adhesive of a buffer/YBCO layer. If the brittle adhesive layer, i.e. buffer/YBCO, is  
6 debonded or fractured, the YBCO conductor performance is substantially degraded.

7 Petrie [11] has listed five basic stress types common to adhesive joints; tensile  
8 stress, shear stress, compressive stress, cleavage stress and peel stress. Tensile  
9 corresponds to the transverse tensile stress. Cleavage occurs when an external force acts  
10 to open one edge of the adhesive assembly. Peel is similar to cleavage, while an  
11 adherend is flexible. In the case of cleavage and peel, the stress is concentrated on a  
12 small part of the adhesive bond and therefore their (cleavage and peel) strengths are  
13 much lower than the tensile strength. Therefore, both cleavage and peel are undesirable  
14 and are usually avoided in the adhesive bond assembly design. [11]

15 Considering the close resemblance between an YBCO-coated conductor and an  
16 adhesive joint assembly, it is probable that cleavage is undesirable in the YBCO-coated  
17 coil. However, so far the effect of cleavage on the YBCO-coated conductor has never  
18 been investigated. This paper is a report of such a study using a model experiment.

1           The topics investigated are (a) effect of cleavage on the critical current of the  
2 YBCO-coated conductor, (b) microstructures of the fracture surface of the  
3 YBCO-coated conductor made by a cleavage experiment and (c) the effect of slit edge  
4 on the cleavage strength of the conductor. Stress concentration in the YBCO-coated  
5 conductor loaded in cleavage is numerically analyzed by finite element software. The  
6 effect of cleavage on the performance of epoxy impregnated YBCO-coated conductor  
7 coil will be discussed.

8

## 9   **2. Experimental procedure**

10           The YBCO-coated conductor manufactured by SuperPower Inc. (SCS4050), 4  
11 mm in width and 0.1 mm in thickness, was used in the experiment. It was utilized by  
12 Ion Beam Assisted Deposited (IBAD) MgO technology for the buffer layer and by  
13 metal organic chemical vapor deposition (MOCVD) for the YBCO layer. The thickness  
14 of the Hastelloy substrate, the buffer layer, the YBCO layer and the silver surface layer  
15 were 50  $\mu\text{m}$ , 0.1-0.2  $\mu\text{m}$ , 1  $\mu\text{m}$  and 2  $\mu\text{m}$  respectively and the conductor was covered  
16 with a 20  $\mu\text{m}$ -thick copper plate as seen in Fig. 1(a). The original YBCO-coated  
17 conductor was slit into several conductors in the manufacturing process that was used in  
18 this experiment. The 4 mm wide conductor used in this experiment had a slit edge on

1 one side and an original edge on another side as seen in Fig. 1(a).

2 Experimental arrangement of the cleavage experiment is shown in Fig. 1(b);  
3 both an upper anvil (copper) and a lower anvil (copper) were soldered onto the  
4 YBCO-coated conductor using a Sn-3.8wt%Cu-1.0wt%Ag solder. The cleavage force is  
5 applied to the right edge of the conductor as seen in Fig. 1(b), acting so as to open the  
6 YBCO-coated conductor. The solder-bonded area was 16 (= 4×4) mm<sup>2</sup>.

7 The apparatus for the cleavage experiment at cryogenic temperature (77 K) is  
8 shown schematically in Fig. 1 (c). An upward force pulls the upper-right end of a lever  
9 arm, loading a cleavage force on the YBCO-coated conductor. This action is generated  
10 and controlled by a pneumatic system installed on top of the apparatus. The cleavage  
11 force is measured by a load cell installed in the pulling rod. The distance between the  
12 pulling rod and the conductor center is 10.8 mm. Displacement of the pulling rod was  
13 measured by a displacement gauge installed on a top flange. An acoustic emission (AE)  
14 sensor was attached to the fiber reinforced plastic base rod on which the lower anvil was  
15 bolted; the AE sensor measures acoustic waves generated by conductor delamination.  
16 Both terminals of the conductor were soldered to current leads connected to a DC power  
17 supply. A pair of voltage taps was attached to the conductor.

18 Several load/unload cycles were repeated; for each cycle, the maximum

1 upward force exceeds the last peak value by a certain amount of force. The load/unload  
2 cycle was repeated until the conductor was completely delaminated. The critical current  
3 for the conductor was measured after unloading the upward force.

4 Fracture surfaces formed by cleavage experiments were examined with a  
5 scanning electron microscope (SEM) and by energy dispersive spectroscopy (EDS).

6

### 7 **3. Experimental results**

#### 8 **3.1 Delamination of the YBCO-coated conductor by cleavage experiments**

9 Figure 2 (a) shows a cleavage force vs. vertical displacement plot; the cleavage  
10 force is applied to the slit-edge of the YBCO-coated conductor. The right-hand vertical  
11 axis gives a corresponding nominal cleavage stress. The nominal cleavage stress is  
12 defined as the cleavage force divided by the area of the solder bond to the upper anvil.  
13 During the 1st run (#1) and the 2nd run (#2), the curve was elastic; i.e. it is reversible  
14 and few AE events appear. The conductor critical current seen in Fig. 2 (c) coincides  
15 with the initial critical current.

16 In the 3rd run (#3), the cleavage force vs. displacement curve shows a bend at  
17 point (A); its cleavage force is 7.0 N corresponding to the nominal cleavage stress of  
18 0.44 MPa. A train of AE events appears simultaneously. During unloading of the



1 cleavage force, the force-displacement curve is linear and no AE event appears. The  
2 critical current decreased to 100 A. Thus, it is clear that delamination of the  
3 YBCO-coated conductor starts to occur above point (A), extending with cleavage force.  
4 The extension stops during unloading of the force.

5         In the 4th run (#4), the cleavage force vs. displacement curve is elastic at first  
6 but upon exceeding the last maximum force of 8 N (i.e. 0.5 MPa) at point (B), intensive  
7 trains of AE events begin to appear and the force-displacement curve shows a steep  
8 bend, becoming nearly horizontal with the cleavage force of 6 N (i.e. the nominal  
9 cleavage stress equals to 0.38 MPa). The behavior lasts to the point (C) seen in Fig. 2  
10 (a), where the conductor is completely delaminated; the critical current at point (C) is  
11 zero.

12         This demonstrates that the YBCO-coated conductor delaminates at a nominal  
13 cleavage stress as low as 0.5 MPa. This remarkable weakness against the cleavage stress  
14 is due to stress concentration on a small part of the YBCO-coated conductor in the case  
15 of cleavage fracture. Note that the nominal cleavage stress defined here might not be  
16 directly comparable to the reported transverse strength[7,10], as the stress concentration  
17 factor in this experiment changes with the length of the lever arm.

### 18 **3.2 Microstructure of the fracture surface formed by cleavage experiments**

1           A picture of a typical fracture surface formed in a cleavage experiment at 77 K  
2 is shown in Fig. 3(a). Tin on the left is due to solder on the copper. Figure 3(b) shows a  
3 microstructure of the fracture surface examined by SEM, while Fig. 3(c) shows EDS for  
4 solder. The fracture surface contains Hastelloy, demonstrating that the  
5 buffer/YBCO/silver/copper layer is stripped off from the Hastelloy substrate by the  
6 cleavage experiment.

7           Based on these results, the mechanism of delamination involved in these  
8 cleavage experiments and seen in Fig. 2 is interpreted as follows:

9   (1) Debonding of the buffer/YBCO/silver/copper layer from the Hastelloy substrate  
10 starts to occur from the slit edge of the conductor where the opening tensile stress is  
11 concentrated. The debonded zone gradually extends with cleavage force, resulting in a  
12 bend in the force-displacement plot at point (A) as seen in Fig. 2(a) and AE pulses as  
13 seen in Fig. 2(b).

14   (2) The cleavage force is concentrated at the copper surface plate as the debonding  
15 progresses to copper plate fracture at point (B) in Fig. 2(a), resulting in a steep bend in  
16 the plot. The fracture line seen in Fig. 3(a) is due to this copper fracture.

17   (3) Striping off the buffer/YBCO/silver/copper layer proceeds with time; vertical YBCO  
18 lines seen in Fig. 3(b) are due to stripping off the layer and the discrete AE pulse trains

1 seen in Fig. 2(b) suggest a stick-slip motion of the process. The layer is completely  
2 removed at point (C) in Fig. 2 (a).

### 3 **3.3 Effect of slit edge of the YBCO-coated conductor on the cleavage strength**

4 Another cleavage experiment was conducted at 77 K where the left edge and  
5 the right edge of the YBCO-coated conductor seen in Fig. 1(b) were reversed; i.e. a  
6 cleavage force was applied to the original edge of the conductor instead of the slit edge.  
7 The cleavage force vs. displacement plot in this case is shown by the brown line in Fig.  
8 4(a), while that for the slit edge by a green line; Figure 4(b) shows AE events in the  
9 former case, i.e. original edge. The brown line is linear elastic at first and abruptly drops  
10 at point (D); the cleavage force at this point is 20 N, corresponding to the nominal  
11 cleavage stress of 1.25 MPa. Prior to reaching point (D), only several AE events appear  
12 as seen in Fig. 4(b) suggesting that debonding of the buffer/YBCO/silver/copper layer  
13 from Hastelloy and fracture of the copper plate occur simultaneously at point (D) as  
14 seen in Fig. 4(a). The nominal cleavage strength, 1.25 MPa, for the original edge of the  
15 YBCO-coated conductor is 2.5-times higher than that, 0.5 MPa, for the slit edge.

16 The cleavage force vs. displacement plot becomes horizontal with a cleavage  
17 force of 6 N (0.38 MPa). Stripping off the buffer/YBCO/silver/copper layer from the  
18 Hastelloy substrate was confirmed by a metallurgical microscope.

1           The abrupt drop at point (D) seen in Fig. 4(a) demonstrates that the cleavage  
2 stress required to strip off the buffer/YBCO/silver/copper layer is several-fold lower  
3 than that required for the initial debonding and copper fracture. In the case of the slit  
4 edge, the difference is small since the cleavage strength is low and therefore an abrupt  
5 drop does not appear as seen in Fig. 2(a). This result suggests that once the stripping  
6 process starts, it propagates easily to reach the end of the fracture.

7           Silver and copper layers were etched off by immersing the YBCO-coated  
8 conductor in a solution of  $\text{NH}_3:\text{H}_2\text{O}_2=1:1$ . [12] The SEM picture taken of the slit-edge of  
9 the conductor is seen in Fig. 5 (a); the slit edge shows a saw-tooth pattern and many  
10 cracks and micro-peels exist, which are made in the slitting process of the conductor.  
11 On the contrary, in the case of the original edge of the conductor as seen in Fig. 5(b), the  
12 edge is smooth and there are no cracks and micro-peels. Thus the extremely low  
13 cleavage strength for the slit edge is due to cracks and micro peels on the edge since  
14 they act to initiate debonding. D. C. van der Laan et al. [7] also reported an effect of the  
15 slit edge on the transverse tensile strength of the YBCO-coated conductor.

16           Figure 6 compares dispersion of the cleavage strengths for original edges and  
17 slit edges of the YBCO-coated conductor at 77 K and at room temperature. The  
18 cleavage strength of the YBCO-coated conductor is shown by the open circle, while the

1 cleavage strength when the debonding occurs at the solder joint between the anvil and  
2 the conductor is shown by  $\times$ . We see wide deviation of the cleavage strength for the  
3 original edge between 77 K and room temperature, although it is several-fold higher  
4 than that for a slit-edge; e.g. the maximum cleavage strength is  $>2.1$  MPa, where the  
5 inequality sign is necessary as the debonding occurs at the solder joint. The result also  
6 demonstrates that if we use an YBCO-coated conductor with original edges on both  
7 sides, the cleavage strength for YBCO-coated conductors will be enhanced, resulting in  
8 more suppression of degradation of the YBCO-coated conductor coil performance due  
9 to excessive cleavage stresses.

10

## 11 **4. Discussion**

### 12 **4.1 Stress concentration under cleavage experiment**

13         Stress distribution in the YBCO-coated conductor under cleavage experiment  
14 was numerically analyzed using finite element software Abaqus; the linear elastic  
15 calculation was made in the stress analysis. A 2D-mesh was generated for a  
16 cross-sectional configuration of the experimental apparatus as shown in Fig. 7(a): The  
17 upward force of 8 N was applied to the upper right end of the lever arm while the  
18 bottom plane of the YBCO-coated conductor was restrained. Contour plot of the normal

1 stress  $\sigma_z$  in the vertical direction under 8 N is also shown in Fig. 7(a); tensile stress  
2 appears on the right edge of the conductor, while compressive stress is on the left edge  
3 of the conductor. Figure 7(b) traces  $\sigma_z$ , vs. horizontal position along the conductor width.  
4 The peak tensile stress appearing on the right edge of the conductor, i.e. at point (E) as  
5 seen in Fig. 7(b), is 12.7 MPa and is 25.4 fold higher than the nominal cleavage stress of  
6 0.5 MPa.

7 Based on the stress concentration factor of 25.4 and cleavage stresses seen in  
8 Fig. 6, the peak stress for the original edge of the conductor is estimated to be in the  
9 range from 30 MPa to >53 MPa. This estimated strength is consistent with the  
10 transverse tensile strength, 40-100 MPa, recently reported by Xie et al.[10]. On the  
11 contrary, based on Fig. 4, the peak stress at point (E) in Fig. 7(b) for the slit edge is in  
12 the range 8 to 13 MPa.

#### 13 **4.2 Effect of cleavage on the performance of YBCO-coated conductor coils**

14 Cleavage stress tends to appear for epoxy impregnated YBCO-coated  
15 conductor double pancake coils; a numerical example is given for thermal stress due to  
16 cool down for an epoxy impregnated double pancake coil. The coil parameters are the  
17 same as for the epoxy impregnated coil described in the previous paper [8]. They are 30  
18 mm in inner diameter, 38 mm in outer diameter, 8 mm in height and have a number of

1 turns of 23×2. The YBCO-coated conductor is 4 mm in width and 0.1 mm in thickness  
2 and the coil form is assumed to be epoxy resin, 3 mm in thickness with inter-layer  
3 insulations of 70 μm thickness. The stress distribution in the coil is calculated by the  
4 finite element software Abaqus. Linear elasticity is assumed in the calculation. The coil  
5 is axis-symmetric. Table 1 lists physical parameters for materials used in the calculation.

6           Figure 8 shows the generated mesh of the double pancake coil and deformed  
7 shape and contour plot of the radial stress,  $\sigma_r$ , due to thermal contraction. Thermal  
8 shrinkage of the coil form pulls the inner layers of the coil winding in the axial direction  
9 (i.e. the  $z$  direction) and in the radial direction (i.e. the  $r$  direction), deforming the inner  
10 layers of the coil as seen in Fig. 8. This results in radial stress concentration on the outer  
11 edge of the inner layers as shown by the orange and yellow colors acting as the cleavage  
12 stress. The local stress intensity is ~70 times larger than the average stress intensity in  
13 the coil which will delaminate the YBCO-coated conductor. The stress concentration  
14 factor is much reduced, if we use a coil form with lower thermal contraction than epoxy  
15 resin or if we remove the coil form after epoxy impregnation.

16           In the previous paper [8], degradation of the performance of an epoxy  
17 impregnated YBCO-coated conductor double pancake coil was interpreted as being due  
18 to excessive radial tensile (i.e. transverse) stress in the coil winding suggesting here that

1 additional stress concentration appearing on the edge of the conductor due to cleavage  
2 and peel stress, developed during epoxy cure, cool down and coil charging, might assist  
3 degradation in YBCO epoxy impregnated coils. More investigations are being made in  
4 this regard.

5           If the YBCO-coated conductor coil is impregnated with paraffin wax,  
6 development of cleavage stress and peel stress is unlikely, since paraffin wax is easily  
7 fractured by the applied stress. This is also the case for dry wound YBCO-coated  
8 conductor coils. Therefore the effect of cleavage stress and peel stress are mostly  
9 negligible for paraffin impregnated YBCO-coated conductor coils and for dry wound  
10 YBCO-coated conductor coils.

11           As discussed above, if we use an YBCO-coated conductor with original edges  
12 on both sides, its cleavage strength will be enhanced, resulting in better suppression of  
13 degradation due to cleavage stress and peel stress for the conductor coils. This is  
14 especially true for epoxy impregnated YBCO-coated conductor coils.

15

## 16 **5. Conclusions**

17           Cleavage strength for an YBCO-coated conductor at 77 K was investigated with  
18 a model experiment. Conclusions are as follows:



1 (a) The nominal cleavage strength for the slit edge of the YBCO-coated conductor is  
2 extremely low typically being 0.5 MPa. This is due to stress concentration on a part of  
3 the conductor in the case of cleavage fracture. Debonding by cleavage stress occurs at  
4 the interface between the buffer layer and the Hastelloy substrate, and after debonding,  
5 the critical current for the YBCO-coated conductor is zero.

6 (b) The cleavage strength for the slit edge of the conductor is several-times lower than  
7 that for an original edge of the conductor. This is due to cracks and micro-peel existing  
8 on the slit edge.

9 (c) Cleavage stress and peel stress should be avoided in the coil winding, as they easily  
10 delaminate the YBCO-coated conductor resulting in substantial degradation of the coil  
11 performance. This is especially true for the epoxy impregnated YBCO-coated conductor  
12 coil. We have demonstrated that the cleavage stress on the coil edge might result in  
13 delamination of the YBCO-coated conductor.

14

## 15 **Acknowledgments**

16 This research was supported by Japan Science and Technology Agency, JST,  
17 under Strategic Promotion of Innovative Research and Development Program.

18

19

## 1   **References**

- 2   1. D. W. Hazelton, Recent developments in YBCO for high field magnet applications,  
3       Presented at 2008 Low Temperature Superconductor Workshop, Tallahassee, Florida,  
4       USA, November 11-13, 2008.
- 5   2. M. Sugano, K. Osamura, W. Prusseit, R. Semerad, T. Kuroda, K. Ito, and T. Kiyoshi,  
6       Reversible strain dependence of critical current in 100A class coated conductor,  
7       *IEEE Trans. Appl. Supercond.* **15**, 2005, 3581-3584.
- 8   3. N. Cheggour, J. W. Ekin, C. C. Clickner, D. T. Verebelyi, C. L. H. Thieme, R.  
9       Freeman and A. Goyal, Reversible axial strain effect and extended strain limits in  
10       Y-Ba-Cu-O coating on deformation-textured substrates, *Appl. Phys. Lett.* **83**, 2003,  
11       4223-4225.
- 12   4. W. Goldacker, J. Kessler, B. Ullmann, E. Mossang, M. Rikel, Axial tensile,  
13       transverse compressive and bending strain experiments on Bi(2223)/AgMg single  
14       core tapes, *IEEE Trans. Appl. Supercond.* **5**, 1995, 1834-1837.
- 15   5. S. L. Bray, J. W. Ekin, and T. Kuroda, Critical-current degradation in  
16       multifilamentary Nb<sub>3</sub>Al wires from transverse compressive and axial tensile stress,  
17       *IEEE Trans. Appl. Supercond.* **3**, 1993, 1338-1341.
- 18   6. A. Otsuka and T. Kiyoshi, High field magnet design under constant hoop stress,

- 1        *IEEE Trans. Appl. Supercond.* **18**, 2008, 1529-1532.
- 2        7. D. C. van der Laan, J. W. Ekin, C.C. Clickner, T. C. Stauffer, Delamination strength  
3        of YBCO coated conductors under transverse tensile stress, *Supercond. Sci. Technol.*,  
4        **20**, 2007, 765-770.
- 5        8. T. Takematsu, R. Hu, T. Takao, Y. Yanagisawa, H. Nakagome, D. Uglietti, T.  
6        Kiyoshi, M. Takahashi, and H. Maeda, Degradation of the performance of a  
7        YBCO-coated conductor double pancake coil due to epoxy impregnation, *Physica C*,  
8        **470**, 2010, 674–677.
- 9        9. T. Takematsu, R. Hu, T. Takao, Y. Yanagisawa, H. Nakagome, D. Uglietti, T.  
10       Kiyoshi, M. Takahashi, and H. Maeda, Degradation of YBCO coil performance due  
11       to epoxy impregnation, Presented at Applied Superconductivity Conference, 4LA-01,  
12       August 1-6, 2010, Washington D.C., USA.
- 13       10. Y. Xie, B. Liebl, S. Soloveichik, L. Hope, D. Hazelton, J. Dackow, R. B. Bucinell, A.  
14       Brown, and V. Selvamanickam, C-axis tensile strength of 2G HTS, Presented at  
15       Applied Superconductivity Conference, 1MA07, August 1-6, 2010 Washington, DC,  
16       USA.
- 17       11. E.M. Petrie, Handbook of adhesives and sealants, Second edition, The McGraw-Hill  
18       Companies, Inc. 2007, pp.107-112

- 1 12. J. Kato-Yoshioka, N. Sakai, S. Tajima, S. Miyata, T. Watanabe, Y. Yamada, N.  
2 Chikumoto, K. Nakao, T. Izumi and Y. Shiohara, Low resistance joint of the YBCO  
3 coated conductor, *Journal of Physics: Conference Series* 43 (2006) 166–169.
- 4 13. N. Cheggour, J.W. Ekin, C. C. Clickner, D. T. Verebelyi, C. L. H. Thieme, R.  
5 Feenstra, A. Goyal, and M. Paranthaman, Transverse compressive stress effect in  
6 Y-Ba-Cu-O coatings on biaxially textured Ni and Ni-W substrates, *IEEE Trans. Appl.*  
7 *Supercond.*, **13**, 2003, 3530-3533
- 8 14. N. Cheggour, J.W. Ekin, C. L. H. Thieme and Yi-Yuan Xie, Effect of fatigue under  
9 transverse compressive stress on slit Y-Ba-Cu-O coated conductor, *IEEE Trans.*  
10 *Appl. Supercond.*, **13**, 2003, 3530-3533.

11

1 **Figure Captions:**

2 **Figure 1.** (a) Configuration of the YBCO-coated conductor manufactured by  
3 SuperPower Inc.; (b) schematic arrangement of the cleavage experiment; (c) schematic  
4 diagram of the apparatus for cleavage experiment at cryogenic temperature (77 K).

5 **Figure 2.** (a) The cleavage force vs. displacement plot. Right vertical axis corresponds  
6 to the nominal cleavage stress, defined as the upward force divided by the  
7 solder-bonded area; the cleavage force is applied to the slit edge of the YBCO-coated  
8 conductor; (b) AE event vs. vertical displacement plot for four consecutive load/unload  
9 cycles of the cleavage force; (c) the critical current vs. displacement plot, where the  
10 critical current is measured after unloading the cleavage force.

11 **Figure 3.** (a) Picture of the fracture surface made by cleavage experiment for  
12 YBCO-coated conductor; the cleavage force is applied to the slit edge of the conductor;  
13 (b) microstructure of the cleavage fracture surface taken by SEM; (c) EDS intensities  
14 for Solder (Sn), YBCO(Ba) and Hastelloy (Ni) on the fracture surface.

15 **Figure 4.** The cleavage force vs. displacement plot for the original edge of the  
16 YBCO-coated conductor (green line) and that for the slit edge of the conductor (brown  
17 line).

18 **Figure 5.** (a) SEM picture of a slit edge of the YBCO-coated conductor and (b) that of

1 an original edge of the YBCO-coated conductor. Both copper plate and silver layer were  
2 etched out, by immersing the conductor in a solution of  $\text{NH}_3:\text{H}_2\text{O}_2=1:1$ .

3 **Figure 6.** Deviation of cleavage strength for the original edge and the slit edge of the  
4 YBCO-coated conductor; the measurements are made at 77 K and room temperature.

5 **Figure 7.** (a) 2D mesh generated for finite element structural calculation and a contour  
6 plot of the normal stress,  $\sigma_z$ , parallel to the vertical direction under a cleavage force of 8  
7 N; (b) normal stress  $\sigma_z$  vs. horizontal position along the conductor width.

8 **Figure 8.** Generated mesh of the stress analysis due to thermal contraction for the  
9 YBCO-coated conductor coil; the deformed shape and contour of the radial stress are  
10 also shown.

11

1 Table caption:

2 **Table 1.** Physical parameters used in the stress analysis

3

Figure 1

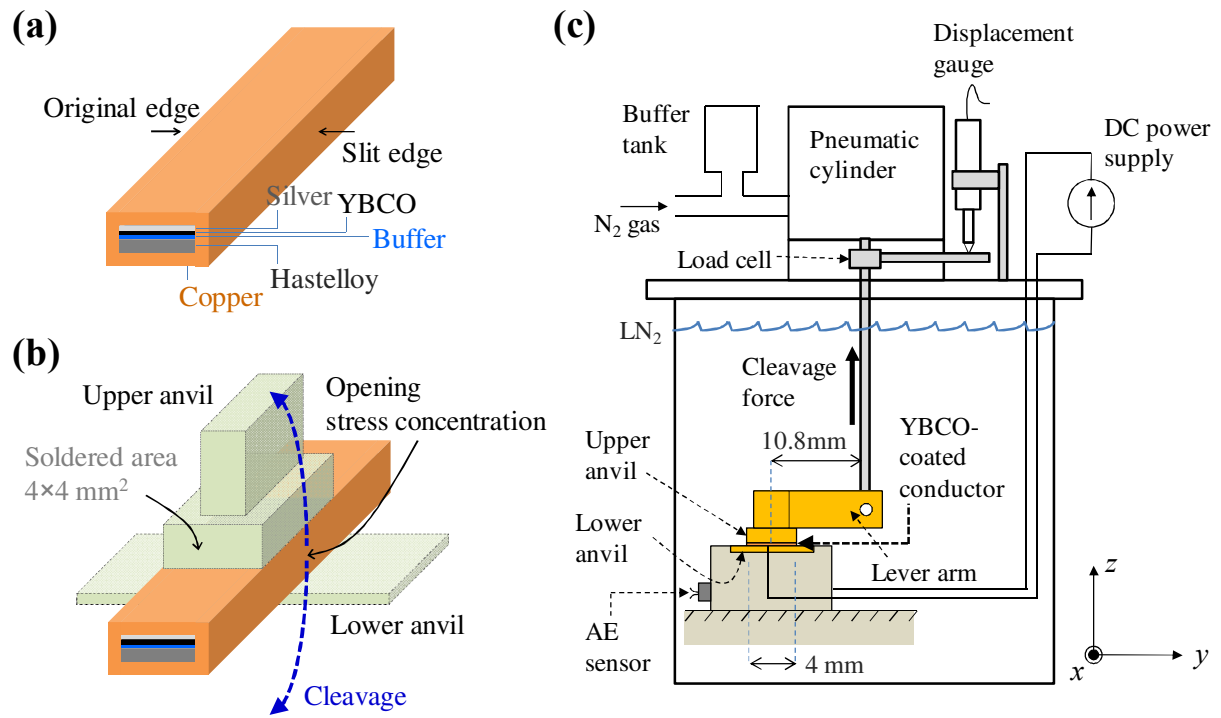




Figure 2

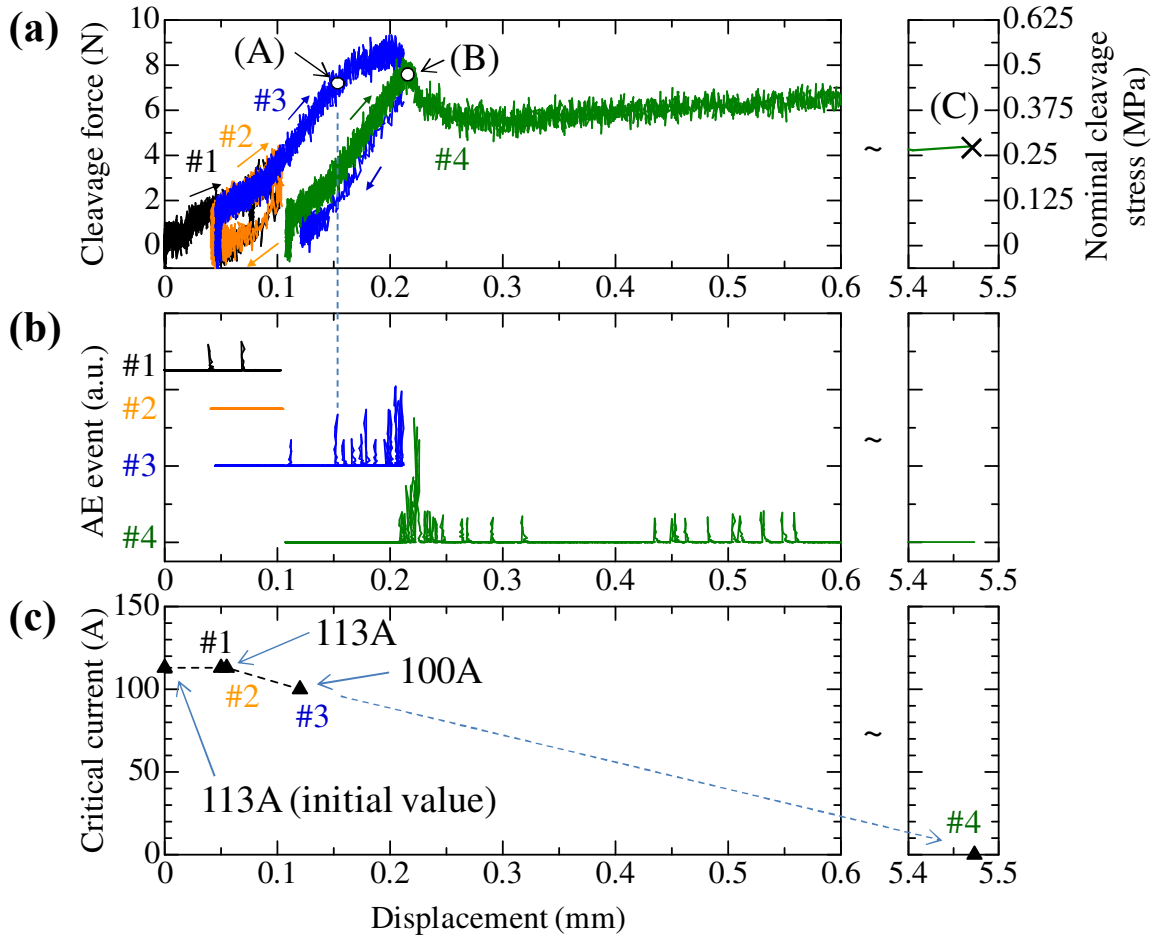


Figure 3

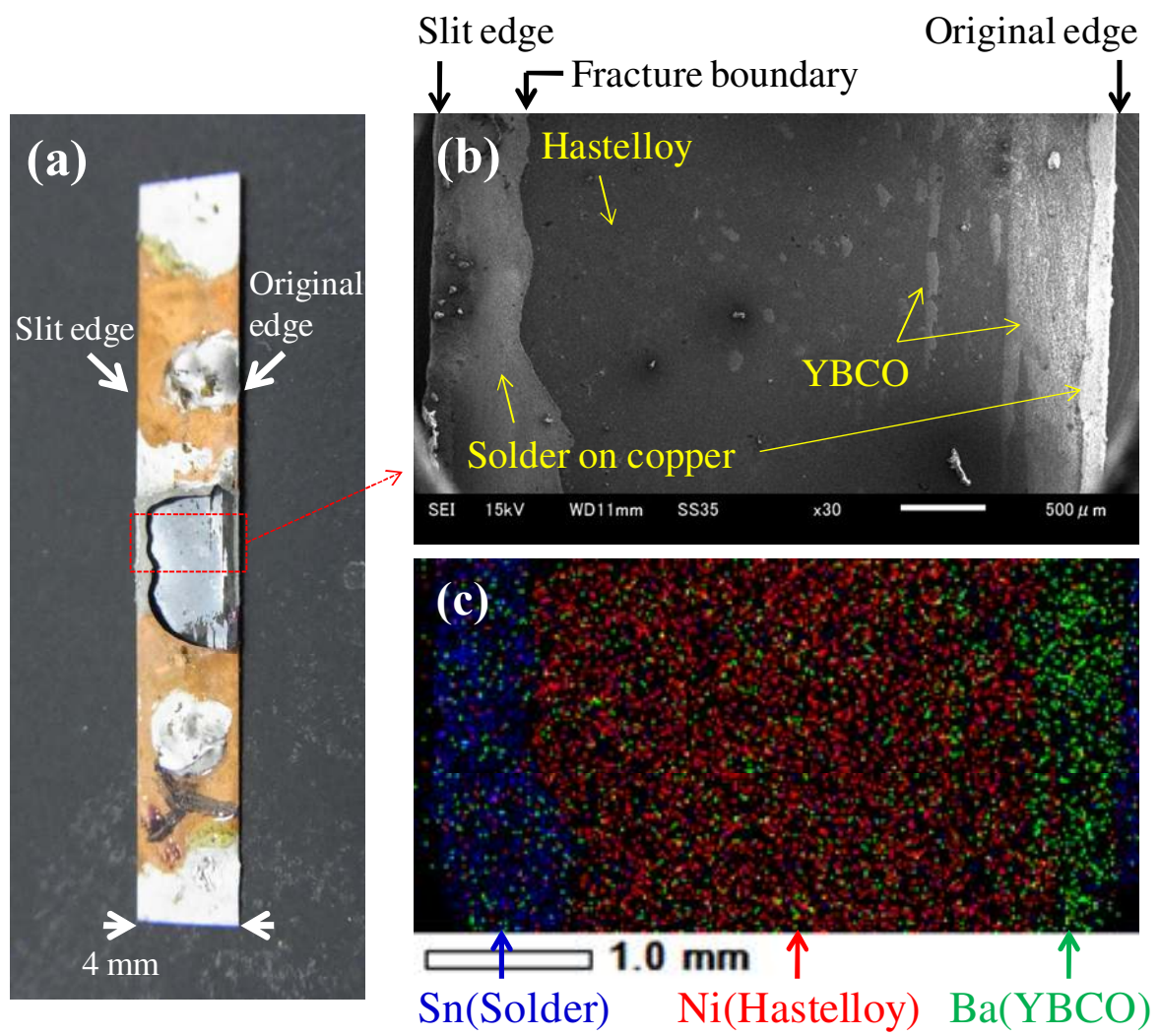


Figure 4

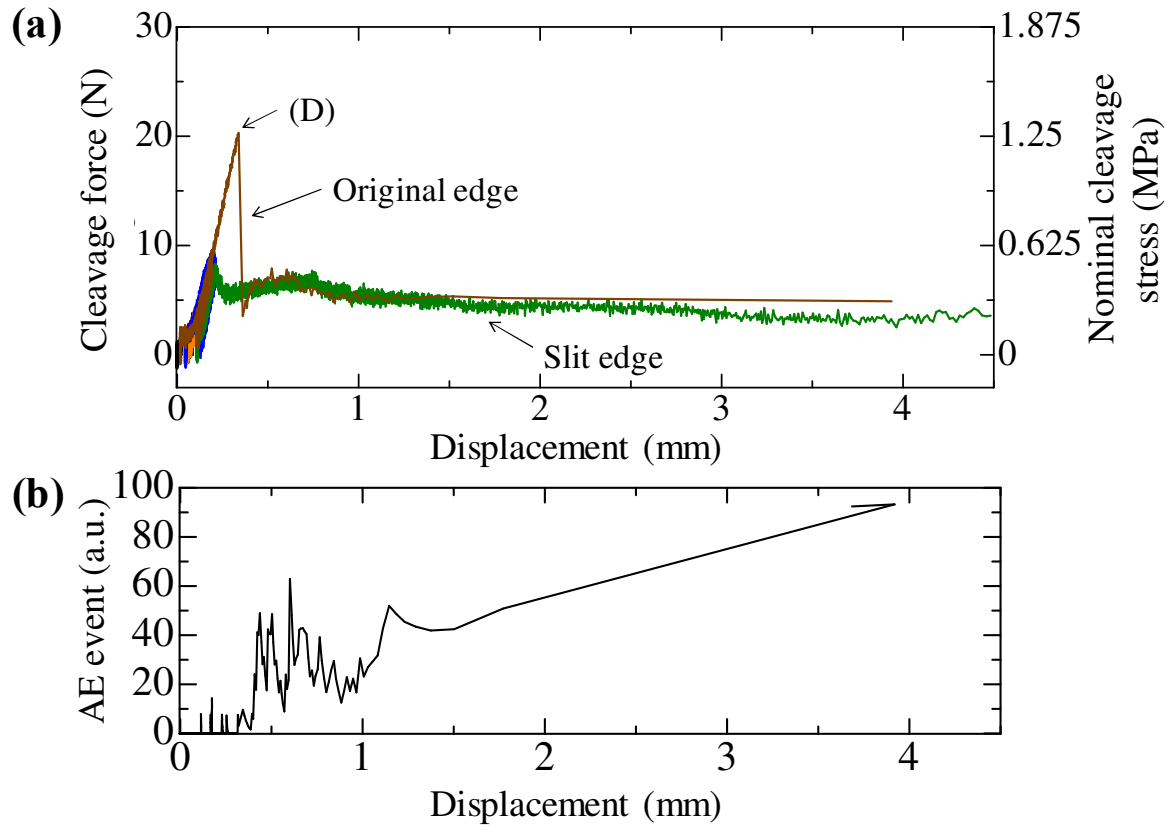
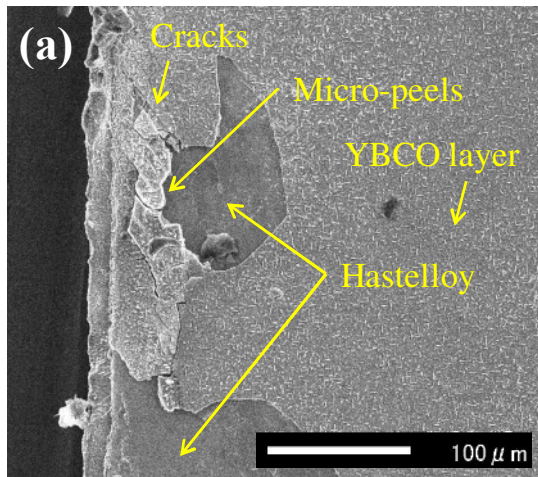
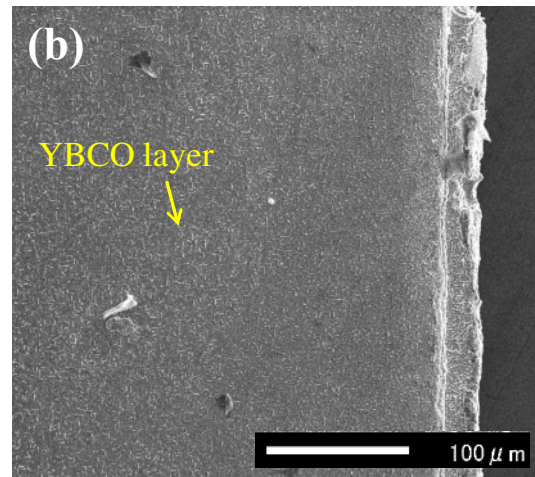


Figure 5



Slit edge



Original edge

Figure 6

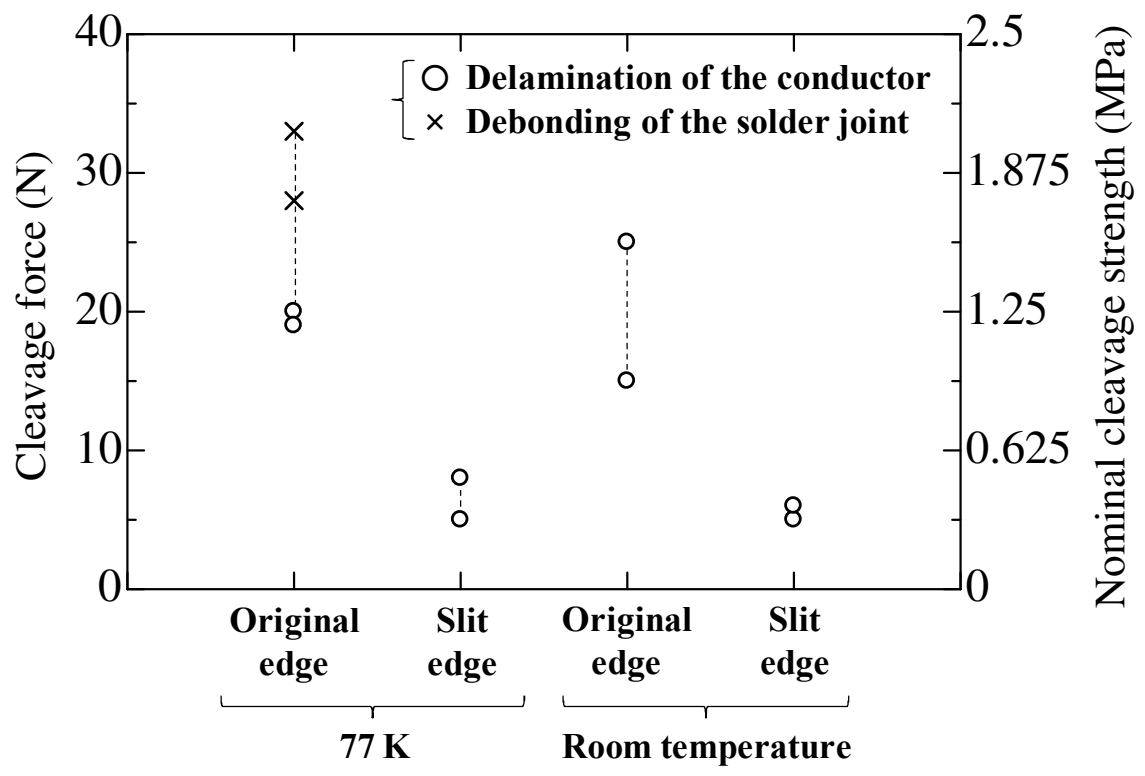


Figure 7

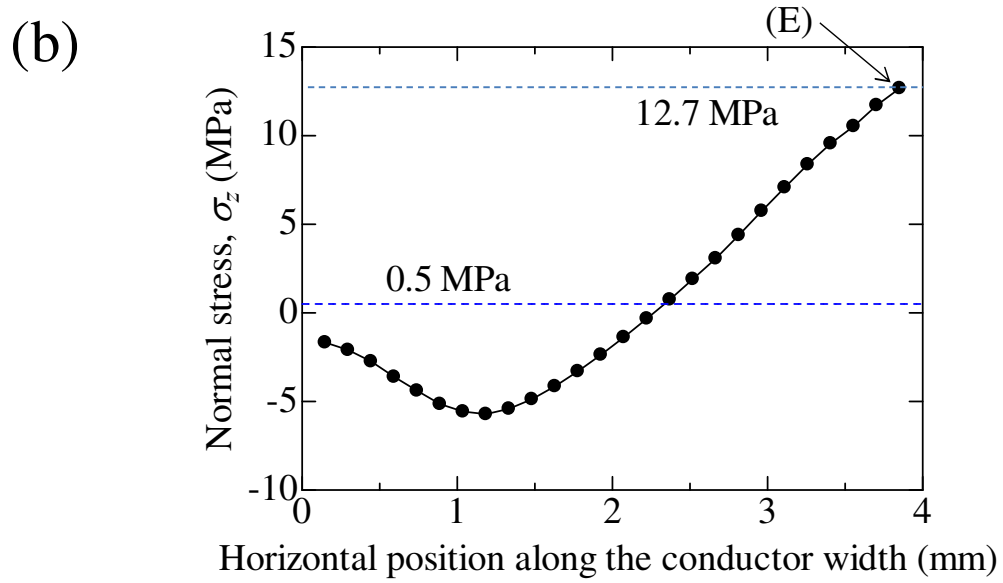
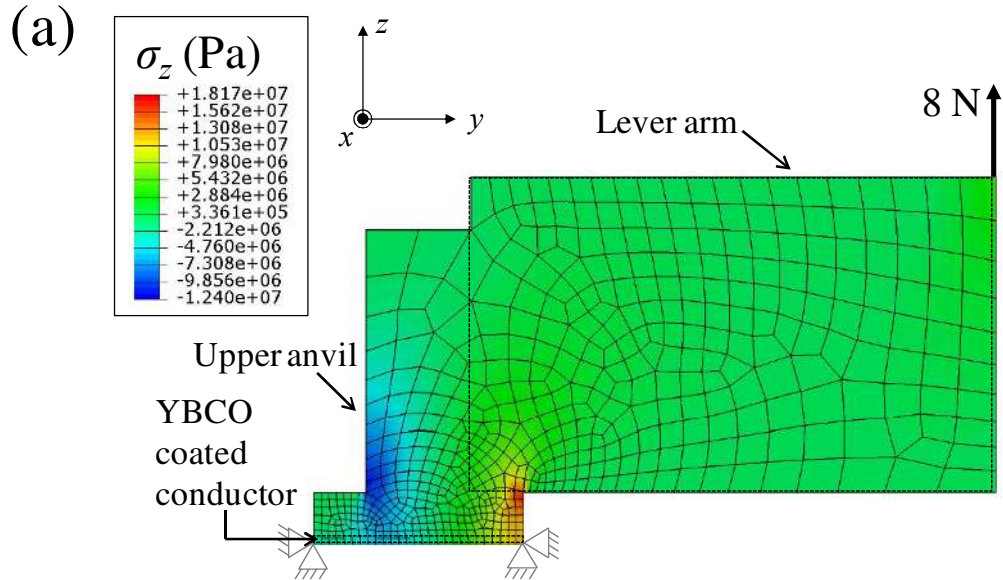


Figure 8

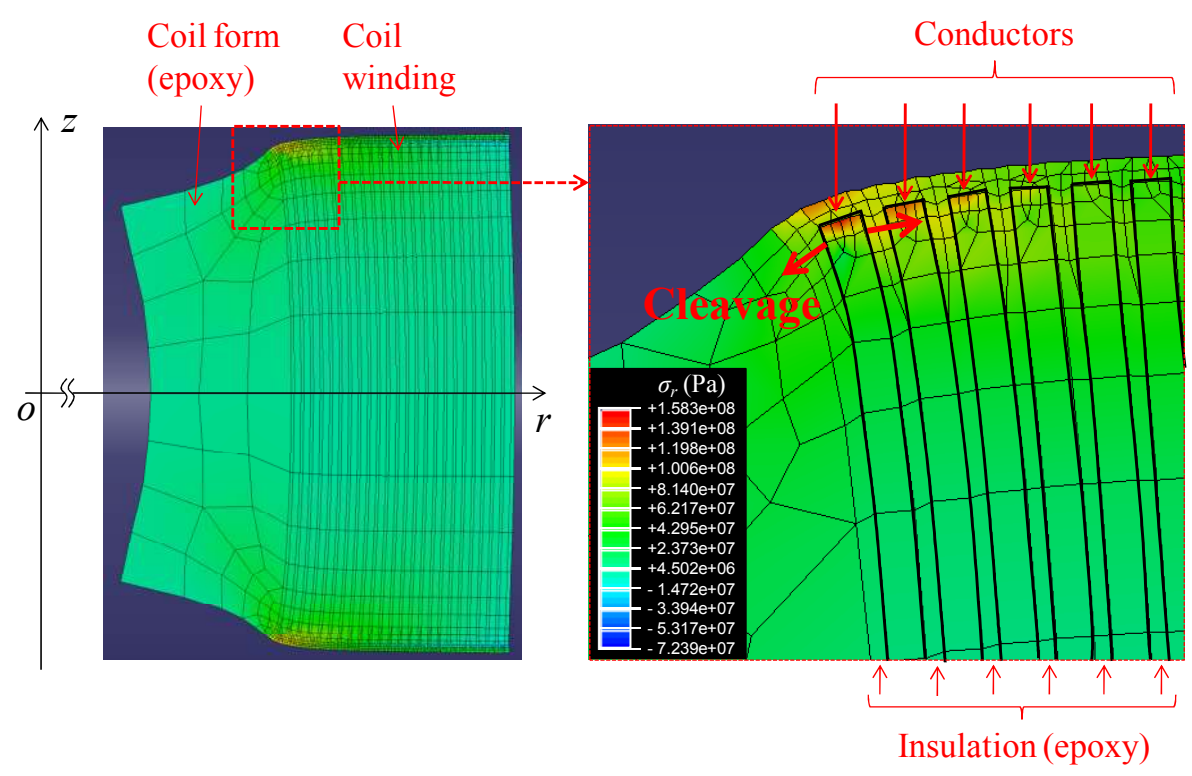


Table 1

Materials	Young's modulus (Pa)	Thermal contraction
YBCO-coated conductor	$2 \times 10^{11}$	-0.00211
Epoxy for coil form and inter layer insulator	$6 \times 10^9$	-0.0102